

Research on the Influence of SCSFCL on Transmission Line Differential Protection

Long Wang¹, Zhuo Chen^{2,*}, Zhenhuan Zhang³, Zhiheng Li¹, Peng Wu¹,
Yinyuan Guo²

¹ Zhengzhou University of Aeronautics, Zhengzhou 450046, Henan China

² Xuchang Kaipu Testing Research Institute Co., Ltd, Xuchang 461000, Henan, China

³ Zhenhuan Zhang, Henan College of Transportation, 450000, Zhengzhou, China

Abstract

The superconducting current limiter plays an important role in limiting the short-circuit current. Therefore, a 500kV iron-core saturated superconducting current limiter (SCSFCL) model was built and its impedance characteristics were analysed. By setting different short circuit faults and then setting different ground resistance at the fault point, different data can be obtained. Finally, the data are summarized. The installation of SCSFCL will not cause the misoperation of current differential protection. In the case of faults in the area, the difference current size at both ends of the line is less affected and the probability of protection rejection is small.

Keywords

Saturated Core Superconducting Fault Current Limiter; The Differential Protection; The Impedance Characteristics; Core Winding; Field Current.

1. Introduction

With the expansion of the power network capacity and topologies become more complex, the short-circuit current in the power system also increases significantly. When a short circuit fault occurs, improper control may lead to serious system stability problems, resulting in greater economic losses and social impact. Saturated core superconducting fault current limiter - SCSFCL has unique engineering advantages. SCSFCL is a nonlinear, time-varying current limiting element, and its impedance characteristics vary greatly in the power network with short circuit fault and without it[1]. During the steady-state operation of SCSFCL, its iron core is in a state of magnetization depth saturation under the combined action of AC and DC magnetic fields on the system side. When the fault occurs, under strong AC action, it works in the linear region and have a high impedance and quickly into the current-limited state. Because the superconducting windings do not have lapse phenomenon in the current limiting process of SCSFCL, there is no lapse recovery and other related problems[2]. In this thesis, based on the analysis of the working principle and operating impedance characteristics of saturated iron core type superconducting current limiter, and a simulation study of the effect of SCSFCL on the correct operation of differential protection of 500kV high-voltage power grid transmission lines is carried out based on the software platform of PSCAD/EMTDC, and analyzes the influence of SCSFCL on differential protection for different high-voltage line short-circuit fault situations[3].

2. How SCSFCL Works

The single-phase SCSFCL model is shown in Figure 1, which consists of a pair of iron-core reactors. Each iron core has a set of superconducting windings and ordinary copper windings, two windings in series with reverse polarity and a strong DC excitation source is attached during normal operation of the SFCL, and make both iron cores in a deep saturation state[4]. At this time, the superconducting current limiter has low impedance. In the event of a high-voltage line fault, the strong AC fault current makes the two iron cores alternately desaturate, at this time, the superconducting current limiter has large impedance, which can serve as a current limiting device. But three-phase SCSFCL usually adopts three-phase six-column loosely coupled structure, and two symmetrical iron cores in the six AC windings of the three-phase SCSFCL are connected to the power network in series, and the overall structure is three-phase and six-core[5]. Part of the internal column is wrapped in DC winding, and the corresponding side is wrapped in AC winding connected to the transmission line for mouth-shaped closed SCSFCL iron core[6].

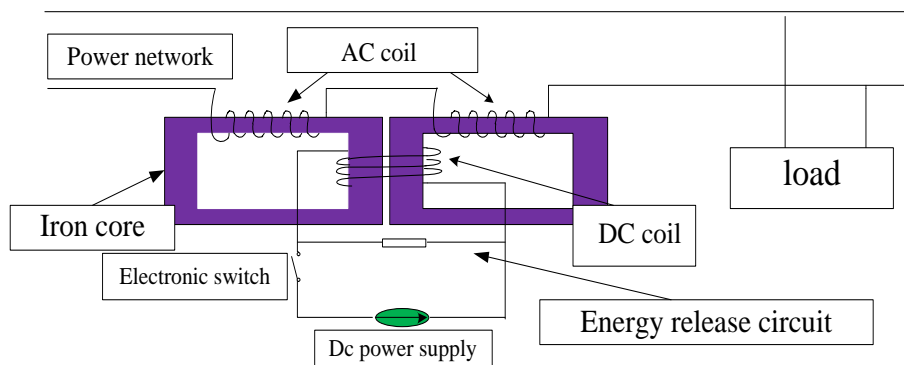


Figure 1. single-item SCSFCL circuit diagram

3. Analysis of SCSFCL Operating Impedance Characteristics

3.1 Modeling of SCSFCL based on PSCAD

The 500kV/3150A SCSFCL designed in this paper is a simulation model based on the information about the latest SCSFCL models currently under research at home and abroad[7]. The magnetic circuit model of the transformer is used to simulate the SCSFCL, and the principle is mainly based on the geometric characteristics of the iron core. main design parameters: power network steady-state voltage 500kV, Steady-state through-current 3150A, effective short-circuit current of the power network 65KA, the effective value of current can be limited 50kA, operating steady-state voltage 5.6kV, Steady-state impedance 2.0Ω, DC winding excitation capacity 580kA. The 500kV [8].single-item SCSFCL model is shown in Figure 2:

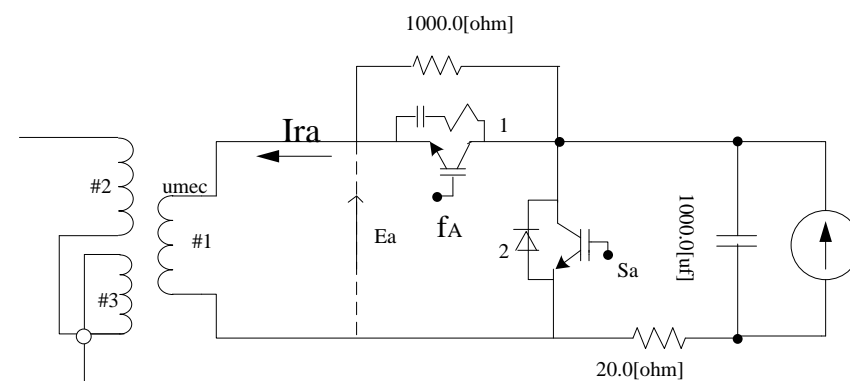


Figure 2. 500kV single-item SCSFCL model

3.2 Analysis of SCSFCL's Operating Impedance Characteristics

The magnitude of the permeability μ of SCSFCL iron core corresponds to the L-I relation of SCSFCL iron core is shown in Figure 3. When the system is short circuited, regardless of whether the fault occurs in the positive or negative half cycle, there is always an iron core of the SCSFCL current limiting coil that immediately enters the linear region with high magnetic permeability from the saturation zone[9-10]. The large inductance can be quickly presented as a large impedance, which can limit the short circuit current. Therefore, the reaction speed of SCSFCL is relatively fast, which is conducive to the operation of relay protection devices such as circuit breakers[11].

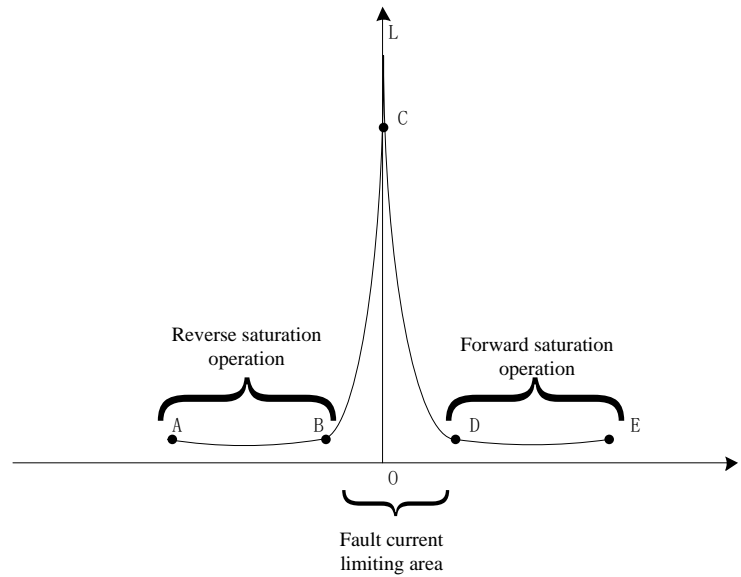


Figure 3. SCSFCL core inductance and current curve

4. Simulation Analysis of Correct Action of transmission Line Differential Protection by SCSFCL

4.1 System Settings

We adopt the differential protection of phase current of industrial frequency[12-15]. The action criterion of current phasor differential protection of transmission line is:

$$|\dot{I}_m + \dot{I}_n| > I_{dz} \quad (1)$$

$$|\dot{I}_m + \dot{I}_n| > k|\dot{I}_m - \dot{I}_n| \quad (2)$$

In the equation, I_m and I_n is the current phasor on the M and N sides of the transmission line shown in Figure 4 and I_{dz} is the operating threshold current of the differential current and k refers to the braking coefficient($0 < k < 1$) [7]. When the currents on the M and N sides of the transmission line satisfy both equations (1) and (2), Protective action makes differential current value $I_{op} = |\dot{I}_m + \dot{I}_n|$ and makes the braking current value $I_{re} = |\dot{I}_m - \dot{I}_n|$. As shown in Figure 4, the set length TL of the line is 150km, the length of the M terminal from the fault point is TL1, and the length of the N terminal from the fault point is TL2.

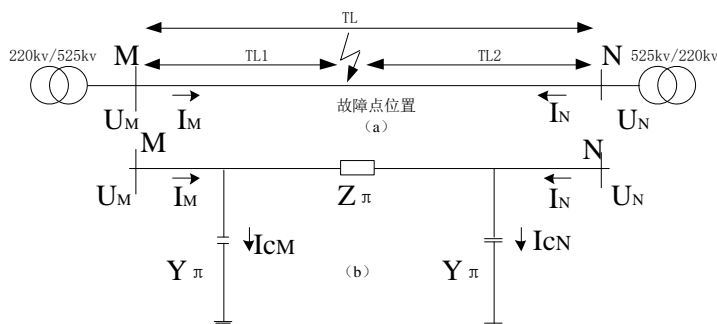


Figure 4. Transmission line schematic

In this electromagnetic simulation, there are four types of faults set at the parallel installation of SCSFCL at the M terminal bus outlet and two types of grounding resistance are set: 0Ω and 20Ω . The simulation model is built on the PSCAD/EMTDC simulation software[16]. The first end (M end) and the end (N end) of the line are respectively set up monitoring points, and the voltage, current and zero sequence current are monitored at the same time. using the discriminatory algorithm of the frequency current change differential relay for analysis[17]. The differential protection discrimination algorithm of power system is shown in Table 1:

Table 1. Differential protection discrimination algorithm

Current differential (phase difference of change) relay	$\begin{cases} \Delta I_{CD\Phi} > 0.75 \times \Delta I_{R\Phi} \\ \Delta I_{CD\Phi} > I_H \\ \Phi = A, B, C \end{cases}$ <p>In the above equation, the power frequency variation differential current is $\Delta I_{CD\Phi}$, $\Delta I_{CD\Phi} = \Delta I_{CD\Phi} + \Delta I_{CD\Phi}$ is the vector and amplitude of current change on both sides of M and N. The braking current of the power frequency variation is $\Delta I_{R\Phi}$, $\Delta I_{R\Phi} = \Delta I_{CD\Phi} + \Delta I_{CD\Phi}$ is the sum of the scalars of the change in current on both sides of M and N.</p> <p>When compensating for capacitive current, I_H is "1.5 times differential current fixed value" and 1.5 times measured capacitor current maximum value; When capacitor current compensation is not put in, I_H is "1.5 times differential current setting" and 4 times measured capacitance current value.</p>
---	--

4.2 Single-phase(A) Earth Fault

When the transition resistance of 0Ω and 20Ω , the data without SCSFCL was compared with that after SCSFCL was added and the use of discriminatory algorithms to analyze the simulation results. The results are obtained as shown in Table 2:

As can be seen from Table 2, when single-phase grounding short-circuit fault occurs, the amplitude of current $|\Delta I_{CD}|$ difference between the two ends of the line does not change much before and after SCSFCL installation. When $TL1=10\text{km}$, $TL2=140\text{km}$ and the ground resistance is 0Ω and 20Ω , the difference of $|\Delta I_{CD}|$ before and after installing SCSFCL is 0.26kA and 0.526kA . When $TL1=75\text{km}$, $TL2=75\text{km}$ and the ground resistance is 0Ω and 20Ω , the difference of $|\Delta I_{CD}|$ before and after installing SCSFCL is 0.02kA and 0.687kA . When $TL1=140\text{km}$, $TL2=10\text{km}$ and the ground resistance is 0Ω and 20Ω , the difference of $|\Delta I_{CD}|$ before and after installing SCSFCL is 0.009kA and 0.902kA .

According to the above data analysis, it is obvious that the farther the short circuit point is from the installation point of SCSFCL, the greater the difference of $|\Delta I_{CD}|$ is, and the maximum difference in the case of single-phase ground short circuit fault is 0.902kA , and according to the differential protection algorithm in Table 1, the installation of SCSFCL will not affect the normal operation of

the current differential protection system[18]. Due to SCSFCL does not add other branches into the line, the addition of SCSFCL has little influence on the differential protection of the line.

Table 2. The line differential protection impedance changes when the single phase (A) grounding

Line(km)	SFCL	current(kA)	Ground impedance 0Ω ΔI _{CD} (kA)	Ground impedance 20Ω ΔI _{CD} (kA)
TL1=10km TL2=140km	Unadd	ΔI _{CD}	13.662	6.598
		ΔI _R	14.223	6.911
	Add	ΔI _{CD}	13.636	6.072
		ΔI _R	14.201	11.735
TL1=75km TL2=75km	Unadd	ΔI _{CD}	12.683	6.318
		ΔI _R	13.312	6.782
	Add	ΔI _{CD}	12.703	5.631
		ΔI _R	13.123	13.133
TL1=140km TL2=10km	Unadd	ΔI _{CD}	17.016	6.780
		ΔI _R	17.620	7.946
	add	ΔI _{CD}	17.025	5.878
		ΔI _R	17.434	15.068

4.3 AB Phase-to-phase Short Circuit Fault

When the transition resistance is 0 Ω and 20 Ω, the data of |ΔI_{CD}| without SCSFCL input is compared with that after SCSFCL input in the line, using the discriminant algorithm to analyze the simulation results, we get the results shown in Table 3:

Table 3. Interphase (AB) circuit differential protection impedance

line(km)	SFCL	current(kA)	Ground impedance 0Ω ΔI _{CD} (kA)	Ground impedance 20Ω ΔI _{CD} (kA)
TL1=10km TL2=140km	Unadd	ΔI _{CD}	13.704	9.672
		ΔI _R	14.097	9.796
	Add	ΔI _{CD}	13.286	9.021
		ΔI _R	16.370	12.934
TL1=75km TL2=75km	Unadd	ΔI _{CD}	14.192	9.666
		ΔI _R	14.666	9.817
	Add	ΔI _{CD}	13.172	8.894
		ΔI _R	17.293	13.683
TL1=140km TL2=10km	Unadd	ΔI _{CD}	18.918	10.641
		ΔI _R	19.531	10.806
	Add	ΔI _{CD}	16.937	9.792
		ΔI _R	22.738	13.912

According to the simulation results in Table 3, it can be seen that when a short circuit occurs between AB phases, the amplitude of the current $|\Delta I_{CD}|$ difference between the two ends of the line before and after switching on SCSFCL does not change much. When TL1=10km, TL2=140km and the ground resistance is 0Ω and 20Ω, the difference of $|\Delta I_{CD}|$ before and after installing SCSFCL is 0.418 kA and 0.651 KA. When TL1=75km, TL2=75km and the ground resistance is 0Ω and 20Ω, the difference of $|\Delta I_{CD}|$ before and after installing SCSFCL is 1.02kA and 0.772KA. When TL1=140km, TL2=10km and the ground resistance is 0Ω and 20Ω, the difference of $|\Delta I_{CD}|$ before and after installing SCSFCL is 1.981kA and 0.849KA.

The analysis of the above simulation results shows that the maximum difference of 1.981kA for $|\Delta I_{CD}|$ occurs when the grounding resistance is 0Ω for AB phase short circuit fault. Although this value is relatively large, the reliability of current differential protection action can be ensured by adjusting the differential protection parameters reasonably when installing SCSFCL. According to the differential protection algorithm in Table 1, the installation of SCSFCL will not affect the normal operation of the current differential protection system.

4.4 AB Phase Indirect Ground Short Circuit Fault

When the transition resistance is 0 Ω and 20 Ω, the data of ΔI_{CD} without SCSFCL input is compared with that after SCSFCL input in the line, using the discriminant algorithm to analyze the simulation results, we get the results shown in Table 4:

Table 4. phase (AB) ground short circuit failure Differential protection impedance changes

line(km)	SFCL	current(kA)	Ground impedance 0Ω $ \Delta I_{CD} $ (kA)	Ground impedance 20Ω $ \Delta I_{CD} $ (kA)
TL1=10km TL2=140km	Unadd	$ \Delta I_{CD} $	15.308	6.643
		$ \Delta I_R $	16.044	7.025
	Add	$ \Delta I_{CD} $	15.434	5.752
		$ \Delta I_R $	17.020	12.702
TL1=75km TL2=75km	Unadd	$ \Delta I_{CD} $	12.902	6.408
		$ \Delta I_R $	7.358	6.901
	Add	$ \Delta I_{CD} $	14.057	5.752
		$ \Delta I_R $	18.058	12.702
TL1=140km TL2=10km	Unadd	$ \Delta I_{CD} $	20.033	6.728
		$ \Delta I_R $	21.391	7.785
	Add	$ \Delta I_{CD} $	19.195	5.852
		$ \Delta I_R $	24.901	14.807

When an AB-phase indirect ground short circuit occurs, the amplitude of the current $|\Delta I_{CD}|$ difference between the two ends of the line before and after switching on SCSFCL does not change much by analyzing the data in Table 4. When TL1=10km, TL2=140km and the ground resistance is 0Ω and 20Ω, the difference of $|\Delta I_{CD}|$ before and after installing SCSFCL is 0.126 kA and 0.891KA. When TL1=75km, TL2=75km and the ground resistance is 0Ω and 20Ω, the difference of $|\Delta I_{CD}|$ before and after installing SCSFCL is 1.155kA and 0.656KA. When TL1=140km, TL2=10km and the ground resistance is 0Ω and 20Ω, the difference of $|\Delta I_{CD}|$ before and after installing SCSFCL is 0.838kA and 0.876KA.

In the case of interphase grounding short circuit, before and after the installation of SCSFCL, the difference of current on both sides of the fault line is very small, not easy to cause the current differential protection rejection, the current differential protection action is reliable. According to the differential protection algorithm in Table 1, the installation of SCSFCL will not affect the normal operation of the current differential protection system[19]. Therefore, SCSFCL installed on transmission lines has little influence on current differential protection.

4.5 ABC Three-phase Short-Circuit Fault

When the transition resistance is 0 Ω and 20 Ω, the data of $|\Delta I_{CD}|$ without SCSFCL input is compared with that after SCSFCL input in the line, using the discriminant algorithm to analyze the simulation results, we get the results shown in Table 5:

Table 5. The impedance change table of ABC three phase short circuit fault

line(km)	SFCL	current(kA)	Ground impedance 0Ω $ \Delta I_{CD} $ (kA)	Ground impedance 20Ω $ \Delta I_{CD} $ (kA)
TL1=10km TL2=140km	Unadd	$ \Delta I_{CD} $	15.486	6.912
		$ \Delta I_R $	15.918	7.177
	Add	$ \Delta I_{CD} $	14.253	6.384
		$ \Delta I_R $	17.447	11.393
TL1=75km TL2=75km	Unadd	$ \Delta I_{CD} $	15.973	6.905
		$ \Delta I_R $	16.478	7.285
	Add	$ \Delta I_{CD} $	14.201	6.201
		$ \Delta I_R $	18.717	12.794
TL1=140km TL2=10km	Unadd	$ \Delta I_{CD} $	21.491	7.189
		$ \Delta I_R $	22.032	8.201
	Add	$ \Delta I_{CD} $	18.768	6.298
		$ \Delta I_R $	25.740	14.867

According to Table 5 above, we can get the three-phase short-circuit fault in transmission line ABC, When TL1=10km, TL2=140km and the ground resistance is 0Ω and 20Ω, the difference of $|\Delta I_{CD}|$ before and after installing SCSFCL is 1.233 kA and 0.528KA. When TL1=75km, TL2=75km and the ground resistance is 0Ω and 20Ω, the difference of $|\Delta I_{CD}|$ before and after installing SCSFCL is 1.772kA and 1.704KA. When TL1=140km, TL2=10km and the ground resistance is 0Ω and 20Ω, the difference of $|\Delta I_{CD}|$ before and after installing SCSFCL is 1.723kA and 0.891KA.

When three-phase short-circuit fault of a transmission line, the three-phase line installed SCSFCL will suppress the short-circuit current, and SCSFCL will not increase the line grounding point, and according to Table 5 of the simulation results, although the fault current is large before and after the installation of SCSFCL, the difference current $|\Delta I_{CD}|$ at both ends of the line will not change significantly [20]. When the grounding resistance is 0 Ω, $|\Delta I_{CD}|$ has a significant change in the line before and after installing SCSFCL, but according to the differential protection algorithm in Table 1, the installation of SCSFCL will not affect the normal operation of the current differential protection system, nor will it cause the current differential protection to reject.

5. Conclusion

- (1) When SCSFCL is connected between the transmission line and the busbar, it will not add ground points in the transmission line and will not cause current differential protection misoperation;
- (2) In the case of a fault within the zone, SCSFCL only limit the size of the line short-circuit current, will not cause changes in the direction of the short-circuit current, after the installation of SCSFCL reasonable adjustment of differential protection parameters can improve equipment reliability and has little impact on the difference current at both ends of the line as a whole;
- (3) From the electromagnetic simulation results and data analysis, it can be seen that the addition of superconducting current limiter has less impact on the power system differential current and causes less probability of protection rejection.

Acknowledgments

Project Information:

- 1) Henan Province Science and Technology Enterprise Cultivation (Science and Technology Little Giant) Special Fund Project (KPJJ-201701);
- 2) Key Project of Science and Technology of Henan Province: Research on Integration and Complementary Technology of Electric Vehicle and Multi-Energy Grid (232102240102);

The research content of this project focuses on the characteristics of electric vehicles, multi-energy power integrated management and vehicle network interactive integration, integration and complementarity, establishing the system integration, integration and complementarity model of electric vehicles, smart grid and distributed power generation, and studying the interactive integration strategy of charging facilities and multi-energy smart grid. The energy scheduling integration mechanism of electric vehicles and multi-energy smart grid will be formulated;

- 3) Key Science and Technology Projects of Henan Province: Vehicle high-beam violation detection and Capturing system, Project No. : 182102310784; The main research is the detection of high beam violation, computer recognition and the research and development of software and hardware system for capturing the relevant information of illegal vehicles;
- 4) Key science and technology projects of Henan Province: 222102240117, Research on fusion technology of electric vehicles, smart grid and distributed power generation: Research content around the electric car, distributed generation, energy storage, power grid interactive integration features, research targets in the safety management and economic operation of energy management and control strategy, set up the electric car with smart grid, a distributed power generation system integration security integration model, study the charging infrastructure and the safety of power grid and distributed generation fusion strategy; Formulate a security integration mechanism for electric vehicles, smart grid and distributed power generation in multiple scenarios.

References

- [1] Wang Long, Song Meng, etc. . Simulation Study of 500 KV saturated iron core type superconducting fault current limiter based on PSCAD. Low temperature and superconductivity, July 2017, vol. 45, no. 7,60-65.
- [2] GUAN Ruiyang, WEI Xinlao, ZHU Bo, et al. Controlled magnetic-wedge linear adjustable reactor[J]. Journal of Harbin University of Science and Technology, 2020,25 (2): 80-87.
- [3] Yacine Ayachi Amor, Gaëtan Didier, Farid Hamoudi et al. Application of a novel approach of resistive-type superconducting fault current limiter with a fast protection system in multi-terminal direct current network[J] International Transactions on Electrical Energy Systems, 2020, 30(10).
- [4] Yacine Ayachi Amor, Gaëtan Didier, Farid Hamoudi et al. Application of a novel approach of resistive-type superconducting fault current limiter with a fast protection system in multi-terminal direct current network[J] International Transactions on Electrical Energy Systems, 2020, 30(10).

- [5] Cao Zhiwei, Ren Li, Yan Sinian, Zhang Yu, Xu Ying, Tang Yuejin, Shi Jing, Li Jingdong. Technical and economic analysis of a 220 kV flux - coupling - type superconducting fault current limiter. *Cryo. & Supercond*, 2020, Vol. 48 ,No. 11.
- [6] N Riva, Riva N, Sirois F et al. Resistivity of REBCO tapes in overcritical current regime: impact on superconducting fault current limiter modeling[J] *Superconductor Science and Technology*, 2020, 33(11).
- [7] LI Bin, WANG Changqi, WEI Ziqiang, et al. Technical requirements of the DC superconducting fault current limiter[J]. *IEEE Transactions on Applied Superconductivity*, 2018, 29(5): 1-5.
- [8] ZHANG Guoming, WANG Haonan, QIU Qingquan, et al. Recent progress of superconducting fault current limiter in China[J]. *Superconductor Science and Technology*, 2021, 34(1).
- [9] LIU Jian, TAI Nengling, FAN Chunju, et al. A hybrid current-limiting circuit for DC line fault in multi-terminal VSC-HVDC system[J]. *IEEE Transactions on Industrial Electronics*, 2017, 64(7): 5595-5607.
- [10] LI Bo tong, CUI Hangqi, JING Fangjie, et al. Current-limiting characteristics of saturated iron-core fault current limiters in VSC-HVDC systems based on electromagnetic energy conversion mechanism[J]. *Journal of Modern Power Systems and Clean Energy*, 2019, 7(2): 411-421.
- [11] Xiang Bin, Cheng Nuo, Yang Kun et al. SF6 passive resonance DC circuit breaker combined with a superconducting fault current limiter[J] *IET Generation, Transmission & Distribution*, 2020, 14(14).
- [12] Song Meng, Lin Zhekan, modeling and simulation of saturated core type current limiter based on ANSYS. *Guangdong Electric Power*, April 2019, volume 32, issue 4.
- [13] QI Weiqiang, TIAN Cuihua, DONG Jianpeng, et al. Study on inter-turn short circuit fault detection method of shunt reactor based on imbalance degree difference[J]. *Power Capacitors & Reactive Power Compensation*, 2019, 40(5): 110-115.
- [14] Li Jin, Tian Mingxing, Liu Yibin, et al. Accurate calculation of current limiting inductance parameters of transformer type controllable reactor [J]. *High voltage apparatus*, 2019, 55 (5): 188-193.
- [15] Zhang Xitian, Zhuang Jinwu, Gao Hailin, et al. Study on forced commutation method of DC hybrid superconducting current limiter [J]. *Power system protection and control*, 2018, 46 (7): 63-67.
- [16] LOU Baolei. Research on key technologies of series resonant type fault current limiters for EHV grid[J]. *Electric Power*, 2017, 50(6): 56-61.
- [17] N Riva, Riva N, Sirois F et al. Resistivity of REBCO tapes in overcritical current regime: impact on superconducting fault current limiter modeling[J] *Superconductor Science and Technology*, 2020, 33(11).
- [18] Yujun Dong, Jiahui Zhu, Defu Wei et al. 10 kV AC test verification of the high temperature superconducting fault current limiter with bias magnetic field[J] *Cryogenics*, 2020.
- [19] Cao Zhiwei, Ren Li, Yan Sinian, Zhang Yu, Xu Ying, Tang Yuejin, Shi Jing, Li Jingdong. Technical and economic analysis of a 220 kV flux - coupling - type superconducting fault current limiter. *Cryo. & Supercond*, 2020, Vol. 48 ,No. 11.
- [20] LIU Yang, WANG Qian, GONG Kang, et al. Transient stability control strategy of microgrid frequency based on SMES[J]. *Power System Protection and Control*, 2018, 46(15): 101-110.